Supplementary information

Distinct roles for host and tumor intrinsic CD155 in control of tumor growth and metastasis

Xian-Yang Li, Indrajit Das, Ailin Lepletier, Venkateswar Addala, Tobias Bald, Kimberley Stannard, Deborah Barkauskas, Jing Liu, Amelia Roman Aguilera, Kazuyoshi Takeda, Matthias Braun, Kyohei Nakamura, Sebastien Jacquelin, Steven W. Lane, Michele W. L. Teng, William C. Dougall, Mark J. Smyth

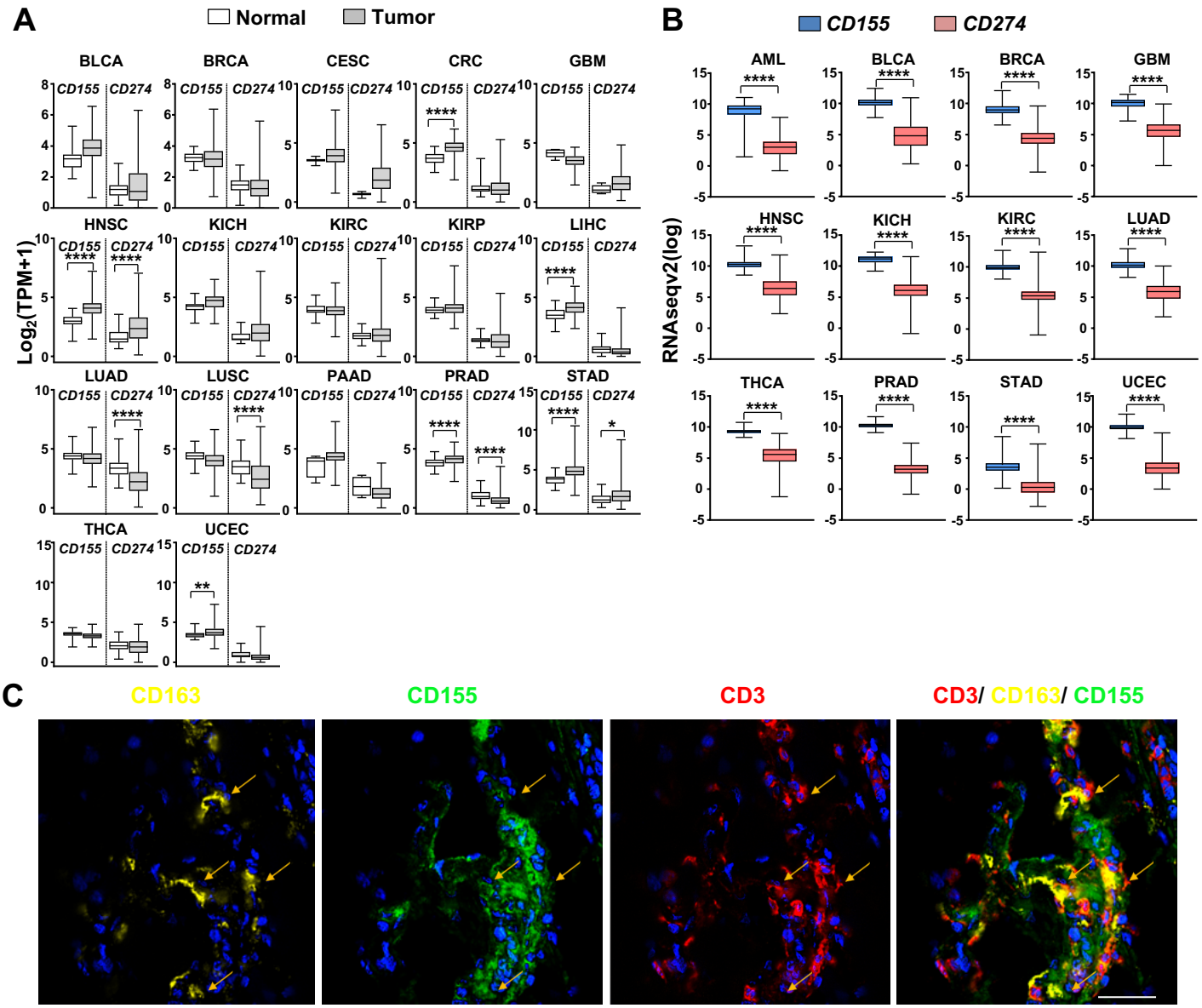
A
Normal
Tumor
BLCA
BRCA
CESC
CRC
GBM
HNSC
KICH
KIRC
KIRP
LIHC
LUAD
LUSC
PAAD
PRAD
STAD
THCA
UCEC
CD155
CD274
Log2(TPM+1)
B
CD155
CD274
AML
BLCA
BRCA
GBM
HNSC
KICH
KIRC
LUAD
THCA
PRAD
STAD
UCEC
RNAseqv2(log)
C
CD163
CD155
CD3
CD3/ CD163/ CD155

Figure S1, related to Figure 1. Expression of human CD155 in host and tumor cells. (A) Gene expression analyses of human cancers were performed as described (Methods and Materials) for all available TCGA data sets and absolute expression (Log2[TPM+1]) of CD155/PVR mRNA and PD-L1/CD274 mRNA were plotted according to tumor vs uninvolved samples. (B) Comparison of absolute mRNA values (RNAseqV2 log) for CD155/PVR mRNA and PD-L1/CD274 from tumor samples demonstrated significantly higher value for CD155 vs. PD-L1 in each cancer type. (C) Representative multiplexed immunohistochemistry (IHC) images of human primary cutaneous melanoma samples. Nuclei were stained blue with DAPI in each panel. Analysis of CD155 expression (green) within infiltrating $CD163^+$ tumor-associated myeloid cells (yellow) in proximity with $CD3^+$ T cells (red), scale bar, 50 μm. CD163+ cells that express CD155 are indicated with yellow arrows.

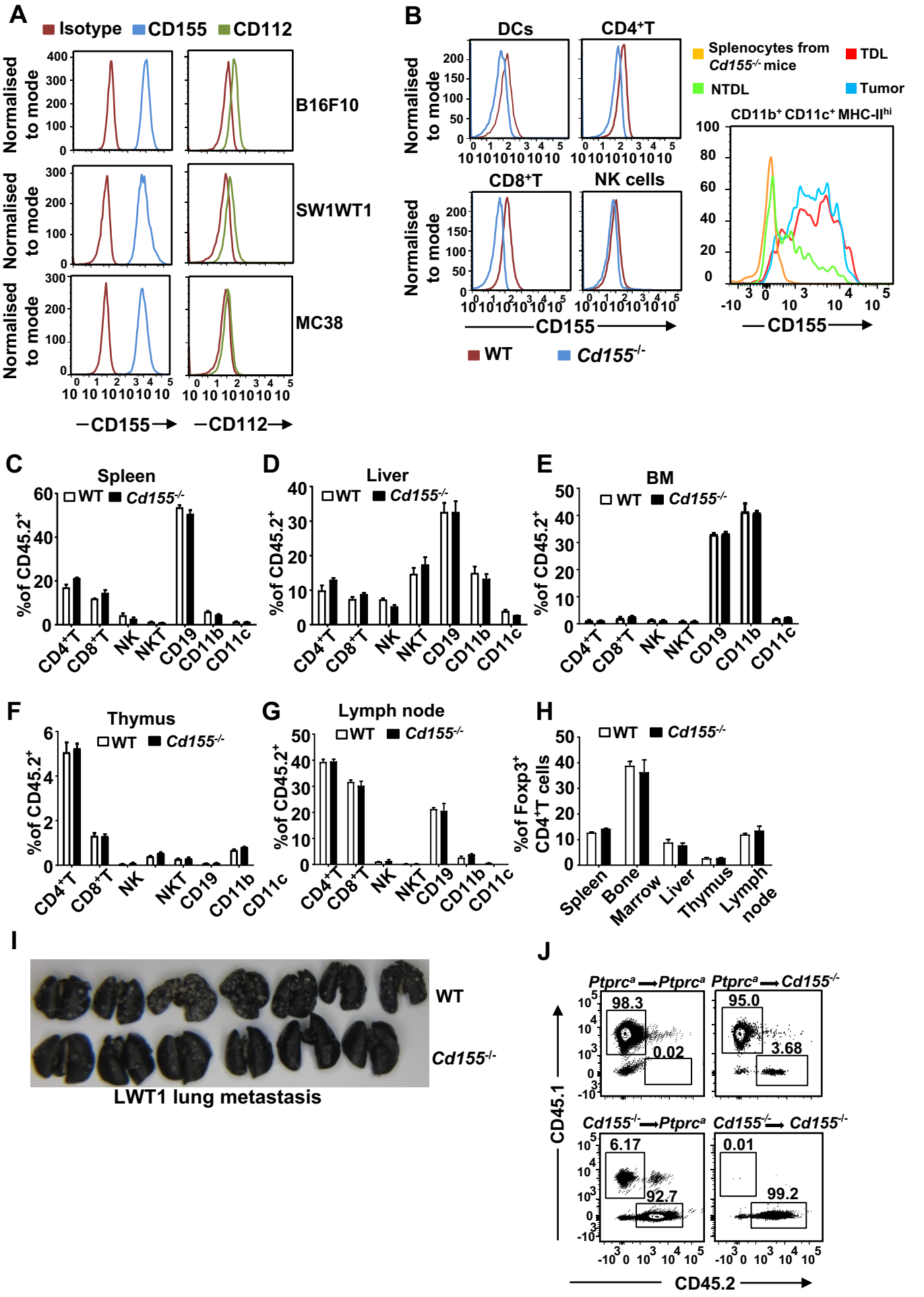
A
Isotype
CD155
CD112
Normalised to mode
B16F10
SW1WT1
MC38
CD155
CD112
B
DCs
CD4+T
CD8+T
NK cells
Splenocytes from Cd155-/- mice
TDL
NTDL
Tumor
CD11b+ CD11c+ MHC-IIhi
CD155
WT
Cd155-/-
C
Spleen
D
Liver
E
BM
%of CD45.2+
CD4+T
CD8+T
NK
NKT
CD19
CD11b
CD11c
F
Thymus
G
Lymph node
H
%of Foxp3+ CD4+T cells
Spleen
Bone Marrow
Liver
Thymus
Lymph node
I
WT
Cd155-/-
LWT1 lung metastasis
J
Ptprca → Ptprca
Ptprca → Cd155-/-
Cd155-/- → Ptprca
Cd155-/- → Cd155-/-
98.3
0.02
95.0
3.68
6.17
92.7
0.01
99.2
CD45.1
CD45.2

Figure S2, related to Figure 1 and 2. CD155 was highly expressed in tumor cells while immune development in CD155$^{-/-}$ mice was largely normal.

(A) CD155 and CD112 expression on B16F10, SM1WT1, and MC38 tumor cells was detected by flow cytometry.

(B) CD155 expression on dendritic cells (DCs), CD4$^+$ T, CD8$^+$ T cells, NK cells from spleens of naïve WT and CD155$^{-/-}$ mice were detected by flow cytometry (left). CD155 expression on CD45.2$^+$/Zombie-yellow$^-$/CD11b$^+$/CD11c$^+$/MHC-II^{hi} cells from B16F10 tumor infiltrating myeloid populations (Tumor) or tumor draining lymph node (TDL) or non-tumor draining lymph node (NTDL) were detected by flow. Splenocytes from *Cd155*$^{-/-}$ mice were shown as negative control (right).

(C-G) The percentages of CD45.2$^+$ immune cells were compared between WT and CD155$^{-/-}$ mice (n=4/group) in spleen (C), liver (D), BM (E), thymus (F), lymph node (G).

(H) Percentage of Foxp3$^+$ CD4$^+$Treg cells was assessed in the indicated organs of WT and *Cd155*$^{-/-}$ mice.

(I) Image of lungs with LWT1 tumor metastases in WT and *Cd155*$^{-/-}$ mice from Figure 2E was shown.

(J) C57BL/6 *Ptprc*^{a} (CD45.1$^+$) and *Cd155*$^{-/-}$ (CD45.2$^+$) mice were irradiated twice (total radiation dose: 1050 cGy/Rads), 5 x 10^6 bone marrow (BM) cells from *Ptprc*^{a} or *Cd155*$^{-/-}$ mice were then i.v. injected to each irradiated mouse to construct BM chimeric mice as described in Figure 2H. Six weeks after BM cell transfer, the reconstitution of BM chimeras was assessed by flow cytometry (Number of mice per experimental cohort, n = 4-10 per group; graph with mean ± SEM, representative of three experiments were shown unless elsewhere mentioned).

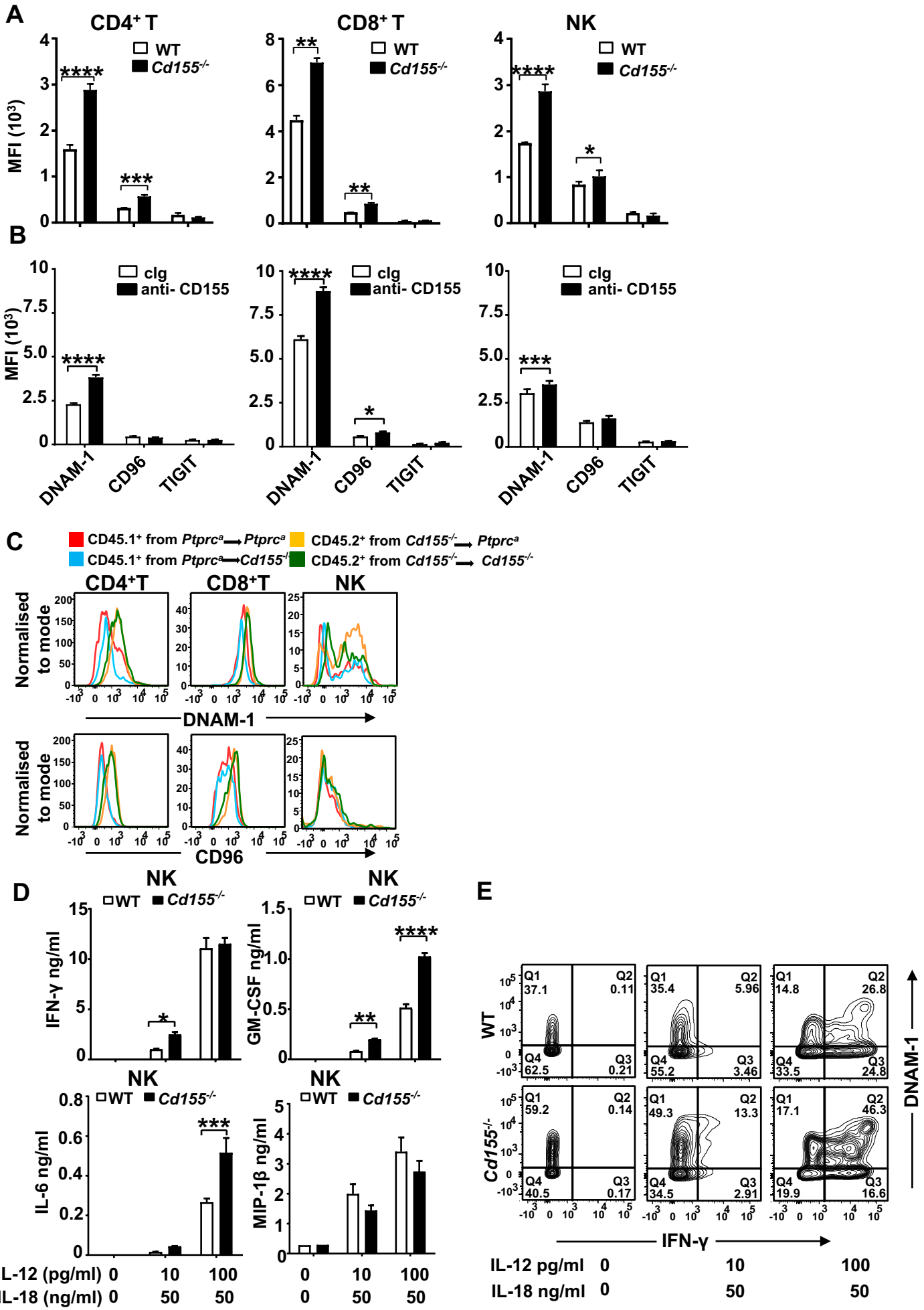
A
CD4+ T
CD8+ T
NK
WT
Cd155-/-
MFI (10³)
B
clg
anti- CD155
DNAM-1
CD96
TIGIT
C
CD45.1+ from Ptprca⟶Ptprca
CD45.2+ from Cd155-/-⟶Ptprca
CD45.1+ from Ptprca⟶Cd155-/-
CD45.2+ from Cd155-/-⟶Cd155-/-
Normalised to mode
D
IFN-γ ng/ml
GM-CSF ng/ml
IL-6 ng/ml
MIP-1β ng/ml
IL-12 (pg/ml) 0 10 100
IL-18 (ng/ml) 0 50 50
E
WT
Cd155-/-
DNAM-1
IFN-γ
IL-12 pg/ml 0 10 100
IL-18 ng/ml 0 50 50

Figure S3, related to Figure 2 and 3. Increased expression of IFN-γ in CD155$^{-/-}$ mice was mediated by DNAM-1 upregulation on immune cells.

(A) DNAM-1, CD96 and TIGIT on CD4$^+$ T, CD8$^+$ T and NK cells from naive splenocytes of wild type (WT) and *Cd155*$^{-/-}$ mice (n=4/group) were analysed by flow cytometry. Mean Fluorescence Intensity (MFI) was shown for each protein on CD4$^+$ T, CD8$^+$ T and NK cells.

(B) DNAM-1, CD96 on CD4$^+$ T, CD8$^+$ T and NK cells from the peripheral blood of C57BL/6 WT mice (n=4/group) were detected by flow cytometry 4 days after i.p. administration of 250 μg of control IgG (1-1) or 250 μg of anti-CD155 (4.24).

(C) Expression of DNAM-1 and CD96 on CD4$^+$ T, CD8$^+$ T and NK cells from the peripheral blood of BM chimeric mice (n=10/group). (D) IFN-γ, GM-CSF, IL-6 and MIP1-β in the supernatant of *in vitro* cultured NK cells were detected with cytokine bead array (CBA) by flow cytometry. (E) Representative flow cytometry data of DNAM-1$^+$ and IFN-γ $^+$ NK cells from WT and *Cd155*$^{-/-}$ mice were shown. (*, $P<0.05$; **, $P<0.01$; ***, $P<0.001$ by one-tailed Mann-Whitney, graph with mean ± SEM, representative of three experiments were shown unless elsewhere mentioned).

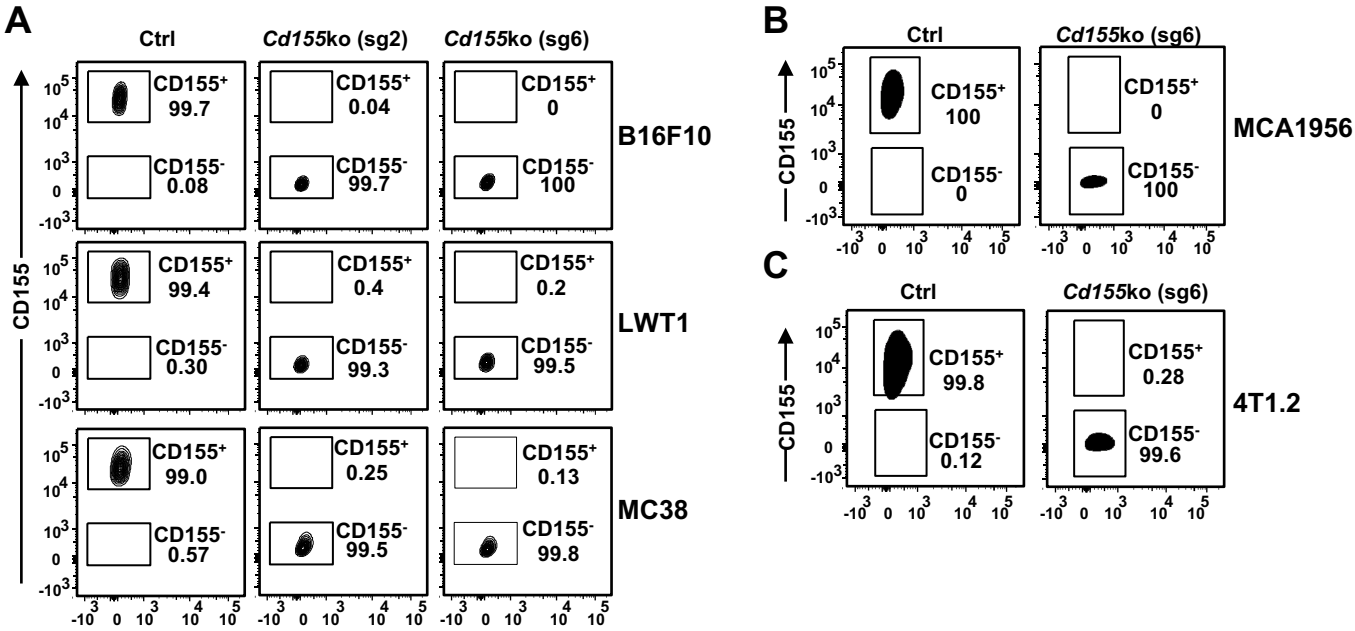
A
Ctrl
Cd155ko (sg2)
Cd155ko (sg6)
CD155
CD155+ 99.7
CD155- 0.08
CD155+ 0.04
CD155- 99.7
CD155+ 0
CD155- 100
B16F10
CD155+ 99.4
CD155- 0.30
CD155+ 0.4
CD155- 99.3
CD155+ 0.2
CD155- 99.5
LWT1
CD155+ 99.0
CD155- 0.57
CD155+ 0.25
CD155- 99.5
CD155+ 0.13
CD155- 99.8
MC38
B
Ctrl
Cd155ko (sg6)
CD155
CD155+ 100
CD155- 0
CD155+ 0
CD155- 100
MCA1956
C
Ctrl
Cd155ko (sg6)
CD155
CD155+ 99.8
CD155- 0.12
CD155+ 0.28
CD155- 99.6
4T1.2

Figure S4, related to Figure 4. Deletion of CD155 on tumor cells using CRISPR-Cas9 system.

(A) B16F10, LWT1, MC38 control and CD155 knockout cell lines were generated by using CRISP-Cas9 system. Representative flow data of CD155 deletion using two guide RNAs, *Cd155*ko (sg2) and *Cd155*ko (sg6) in B16F10, LWT1, MC38 were shown.

(B-C) Deletion of *Cd155* on MCA1956 (B) and 4T1.2 (C) by using CD155 guide RNA *Cd155*ko (sg6) were shown.

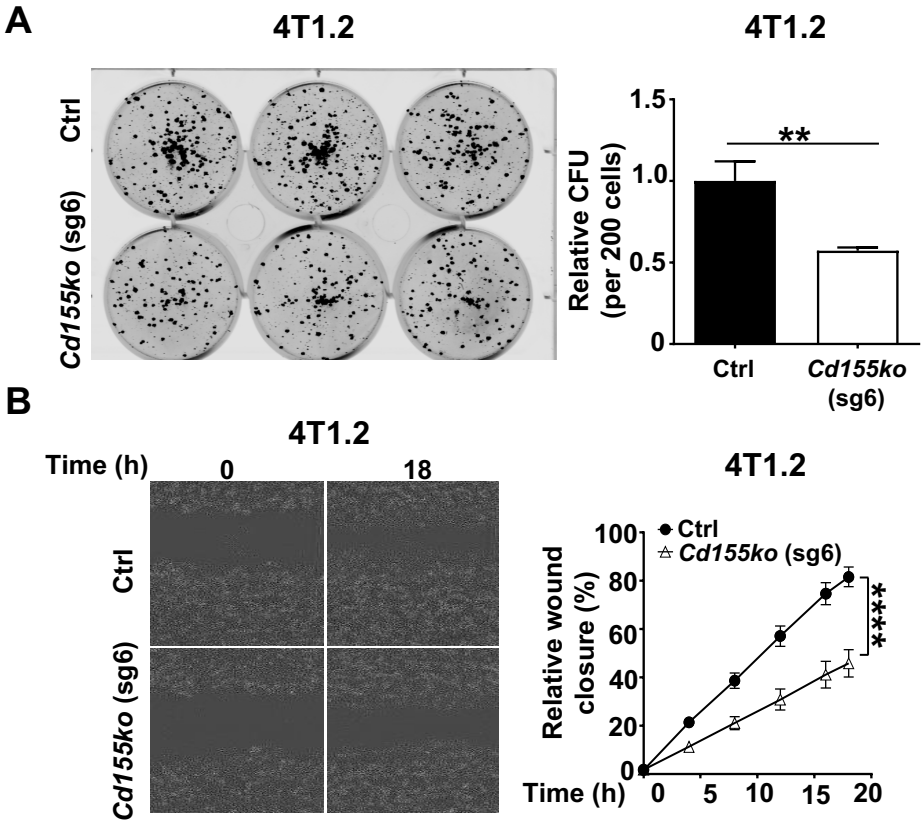
A
4T1.2
Ctrl
Cd155ko (sg6)
4T1.2
Relative CFU (per 200 cells)
1.5
1.0
0.5
0
**
Ctrl
Cd155ko (sg6)
B
4T1.2
Time (h)
0
18
Ctrl
Cd155ko (sg6)
4T1.2
Relative wound closure (%)
100
80
60
40
20
0
Ctrl
Cd155ko (sg6)
****
Time (h)
0
5
10
15
20

Figure S5, related to Figure 5. Deletion of CD155 on 4T1.2 breast cancer cells inhibited colony formation and delayed wound healing *in vitro.*

(A) 200 cells/ well of 4T1.2-Ctrl and 4T1.2-*Cd155*ko (sg6) cells were cultured in 6 well plates for 6 days and stained with crystal violet to assess the relative CFU. The images of the colonies of 4T1.2-Ctrl and 4T1.2-*Cd155*ko (sg6) cells were shown and the relative CFU was assessed.

(B) 4T1.2-Ctrl and *Cd155*ko (sg6) cells were cultured in 96 well plates. Wounds were made with a Scratch Wound Maker and wound healing images were monitored and analyzed by incucyte and percentage of relative wound closure was shown. (**, $P<0.001$, ***, $P<0.001$, ****, $P<0.0001$ by one-tailed Mann-Whitney, graph with mean ± SEM, representative of three experiments were shown).

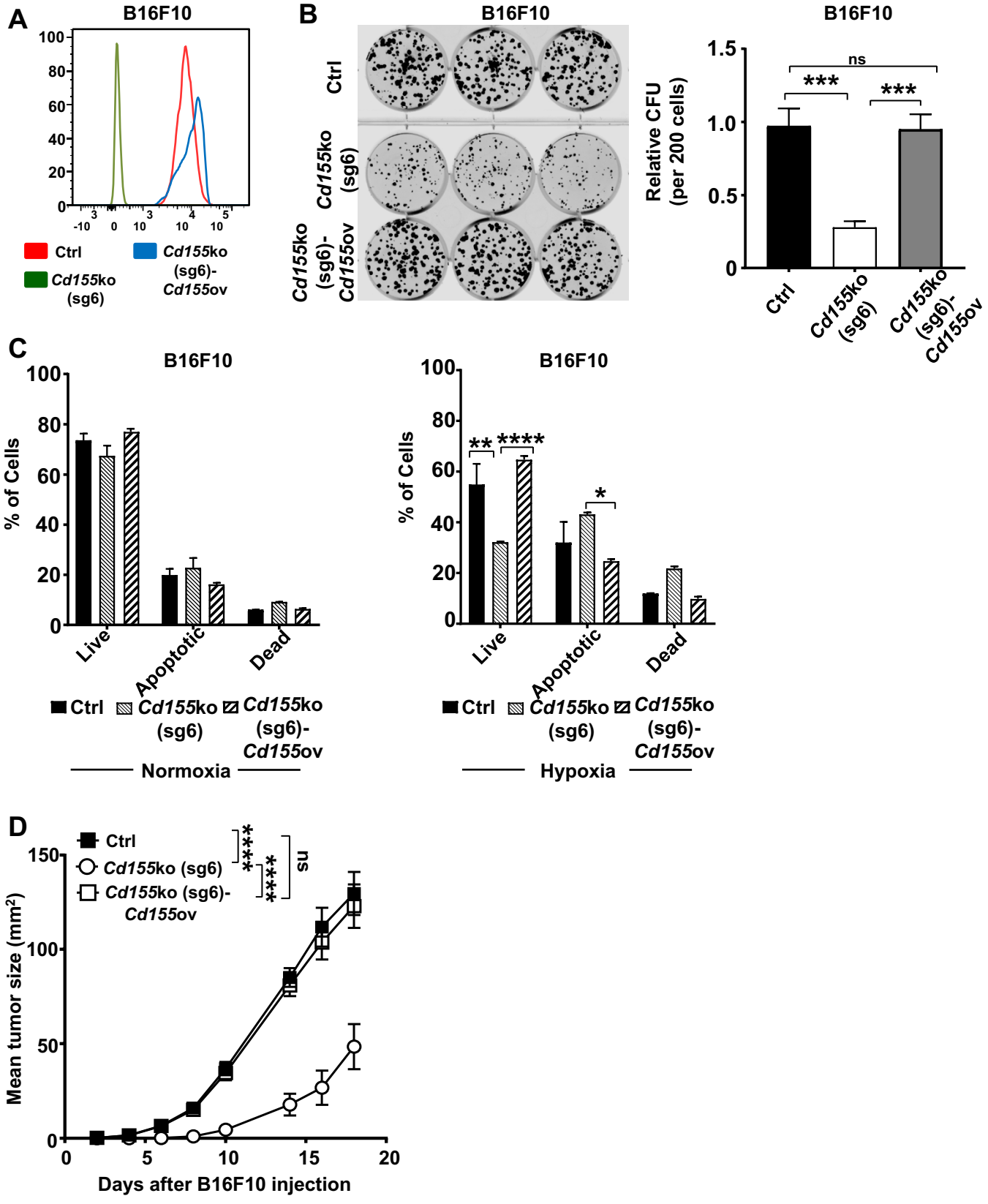
A
B16F10
Ctrl
Cd155ko (sg6)
Cd155ko (sg6)-Cd155ov
B
B16F10
Ctrl
Cd155ko (sg6)
Cd155ko (sg6)-Cd155ov
B16F10
Relative CFU (per 200 cells)
ns
***
***
C
B16F10
% of Cells
Live
Apoptotic
Dead
Normoxia
Hypoxia
**
****
*
D
Mean tumor size (mm²)
Days after B16F10 injection
****
****
ns

Figure S6, related to Figure 5. Overexpression of Cd155 in *Cd155*ko (sg6) reverts tumor cell intrinsic function.

(A) CD155 expression level was detected by flow cytometry in B16F10-Ctrl, B16F10-*Cd155*ko (sg6) and B16F10-*Cd155*ko (sg6)-*Cd155*ov cells.

(B) 200 cells/ well of B16F10-Ctrl, B16F10-*Cd155*ko (sg6) and B16F10-*Cd155*ko (sg6)-*Cd155*ov cells were cultured in 6 well plates for 6 days and stained with crystal violet to assess the relative CFU. The images of the colonies of B16F10-Ctrl, B16F10-*Cd155*ko (sg6) and B16F10-*Cd155*ko (sg6)-*Cd155*ov cells were shown. (***, $P < 0.01$ by one-way ANOVA; graph with mean ± SEM, representative of two experiments were shown).

(C) 1 x 10^5 cells/well of B16F10-Ctrl, B16F10-*Cd155*ko (sg6) and B16F10-*Cd155*ko (sg6) *Cd155*ov were cultured in 24 well plates in normal (normoxic) or hypoxic conditions, and apoptosis were evaluated 48 hrs later with Annexin-V and 7-AAD. Representative rate of cell death was shown in the graphs (C). (*, $P < 0.05$; **, $P < 0.01$; ****, $P < 0.0001$, by one-tailed Mann–Whitney test two-way ANOVA; graph with mean ± SEM, experiments were shown twice).

(D) WT mice were injected s.c. with 1 x 10^5 B16F10-Ctrl or B16F10-*Cd155*ko(sg6) or B16F10-*Cd155*ko(sg6)-*Cd155*ov and tumor size was measured at indicated time points.

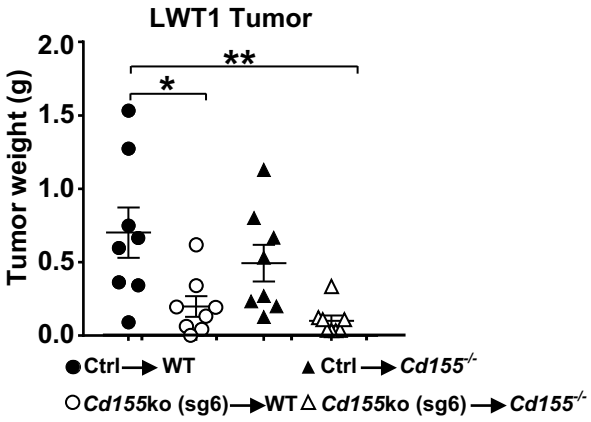
LWT1 Tumor
Tumor weight (g)
2.0
1.5
1.0
0.5
0.0
**
*
Ctrl → WT
Ctrl → Cd155-/-
Cd155ko (sg6) → WT
Cd155ko (sg6) → Cd155-/-

Figure S7, related to Figure 6. Host and tumor CD155 combine to regulate tumor development.

WT and Cd155$^{-/-}$ mice 5 x 10^5 LWT1-Ctrl or LWT1-*Cd155*ko (sg6) cells (n=8-9/group). Tumors were collected at day 14 and tumor weights were shown. (*, $P < 0.05$; **, $P < 0.01$ by two way ANOVA; graph with mean ± SEM, representative of three experiments were shown).

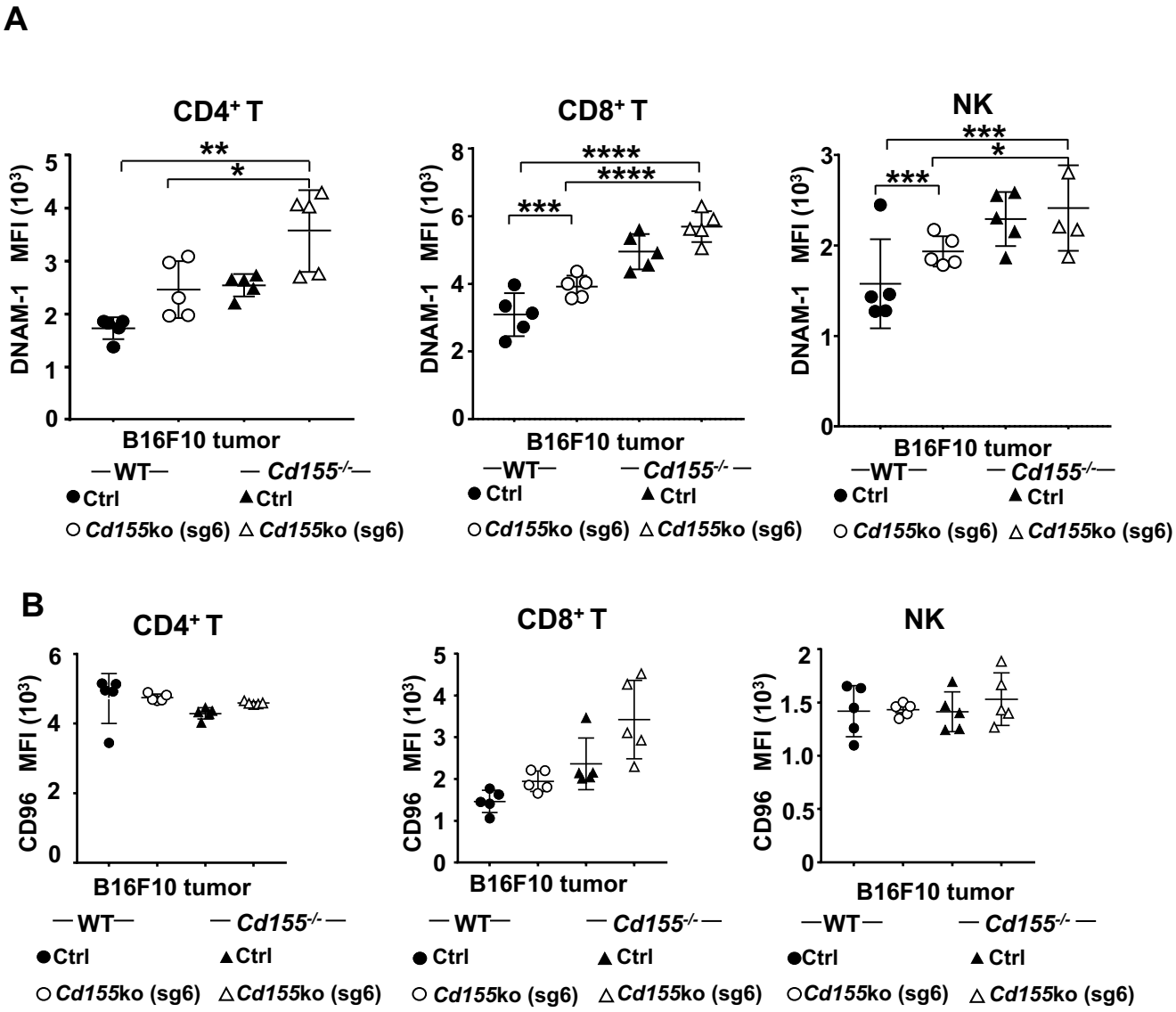
A
CD4+ T
CD8+ T
NK
DNAM-1 MFI (10³)
B16F10 tumor
—WT—
— Cd155-/- —
Ctrl
Ctrl
Cd155ko (sg6)
Cd155ko (sg6)
B
CD96 MFI (10³)

Figure S8, related to Figure 6. Both host and tumor CD155 regulates DNAM-1 expression on immune cells.

(A) DNAM-1 in tumor infiltrating $CD4^+$ T, $CD8^+$ T and NK cells were detected by flow cytometry. The MFI values of DNAM-1 in the treatment groups were shown.

(B) CD96 in tumor infiltrating $CD4^+$ T, $CD8^+$ T and NK cells were by flow cytometry. The MFI values of CD96 in the treatment groups were shown (*, $P < 0.05$; **, $P < 0.01$; ***, $P < 0.001$; ****, $P < 0.0001$ by two-way ANOVA; graph with mean $\pm$ SEM, representative of three experiments were shown unless elsewhere mentioned.

Supplementary Information

REAGENT or RESOURCE	SOURCE	IDENTIFIER
Antibodies		
PerCP/Cy5.5 hamster anti-TCRβ (H57-597)	Biolegend	Cat# 109228; RRID: AB_1575173
APC rat anti-CD8α (53-6.7)	Biolegend	Cat# 100712; RRID: AB_312751
Alexa Fluor® 488 rat anti-CD8α (53-6.7)	Biolegend	Cat# 100723; RRID: AB_389304
Alexa Fluor® 488 anti-mouse CD4 Antibody (RM4-5)	Biolegend	Cat# 100529; RRID: AB_389303
PE anti-mouse NK1.1 (PK136)	Biolegend	Cat# 108708; RRID: AB_313395
APC anti-mouse CD19 Antibody (6D5)	Biolegend	Cat# 115511; RRID: AB_313646
Mouse Nectin-2/CD112 APC-conjugated Antibody (829038)	R&D systems	Catalog #: FAB3869A
PE anti-mouse CD155 (PVR) Antibody (TX56)	Biolegend	Cat# 131507 RRID: AB_1279109
APC anti-mouse CD155 (PVR) Antibody (TX56)	Biolegend	Cat# 131509 RRID: AB_10640453
PE anti-mouse CD226 (DNAM-1) Antibody (10E5)	Biolegend	Cat# 128805 RRID: AB_1186120
APC anti-mouse CD226 (DNAM-1) Antibody (TX42.1)	Biolegend	Cat# 133619
APC anti-mouse IFN-γ Antibody (XMG1.2)	Biolegend	Cat# 505809 RRID: AB_315403
PE anti-mouse CD96 (TACTILE) Antibody (3.3)	Biolegend	Cat# 131705
ANNEXIN V : FITC APOPTOSIS DETECTION KIT I	BD Bioscience	Cat# 556547
7-AAD Staining Solution	BD Bioscience	Cat# 559925
Zombie Yellow™ Fixable Viability Kit	Biolegend	Cat# 423104
Purified anti-mouse CD3ε (145-2C11)	Biolegend	Cat#100302;RRID: AB_312667
APC rat anti-CD11b (M1/70)	Biolegend	Cat# 101212; RRID: AB_312795
eFluor450 anti-Gr-1 (RB6-8C5)	Thermofisher	Cat# 48-5931-82; RRID: AB_1548788
eFluor450 rat anti-CD45.1 (A20)	Thermofisher	Cat# 48-0453-82; RRID:AB_1272189
APC-eFluor 780 rat anti-CD45.2 (30-F11)	Thermofisher	Cat# 47-0451-82; RRID: AB_1548781
Anti-CD45.2-PE-Vio770 (104-2)	Miltenyi	Cat# 130-105-173
FITC anti-mouse CD11c Antibody (N418)	Biolegend	Cat# 117305 RRID: AB_313774
MHC Class II (I-A/I-E) Monoclonal Antibody (M5/114.15.2), APC	eBioscience™	Cat# 17-5321-82
PE anti-mouse/rat/human FOXP3 Antibody (150D)	Biolegend	Cat# 320007 RRID: AB_492981
APC anti-mouse TIGIT (Vstm3) Antibody	Biolegend	Cat# 142105 RRID: AB_10960139
Anti-human PVR/CD155 (D3G7H) Rabbit mAb	CST	Cat# 13544

Anti-human CD11c (EP1347Y) Rabbit mAb	Abcam	Cat# ab52632
Anti-human CD14-(EPR3653) Rabbit mAb	Abcam	Cat# ab133335
Anti-human melanoma marker (HMB45) Mouse mAb	Enzo Life Sciences	Cat# ENZ-C34930
Anti-human PD-L1 (E1L3N®) XP® Rabbit mAb	CST	Cat# 51926s
(A0452) CD3	DAKO	Cat# A0452
CD163 (10D6)	Biocare Medical	Cat# CM353
PE Mouse IgG1, κ Isotype Ctrl Antibody (MOPC-21)	Biolegend	Cat# 400111
APC Mouse IgG1, κ Isotype Ctrl (FC) Antibody (MOPC-21)	Biolegend	Cat# 400121
Anti-mouse CD4 (GK1.5)	Bio X cell	Cat# BE0003-1
Anti-mouse CD8β (Lyt 3.2) (53-5.8)	Bio X cell	Cat# BE0223
Anti-asialoGM1 rabbit polyclonal Antibody	Wako Chemicals USA Inc.	Cat# 986-10001
Rat IgG_{2a} isotype control (1-1)	Leinco Technologies, Inc.	Cat# I-1177
Purified anti-mouse CD155 (PVR) Antibody (4.24)	Biolegend	Cat# 132202
Purified anti-mouse CD226 (DNAM-1) Antibody (480.1)	Biolegend	Cat# 132004
anti-mouse PD-1 (CD279) (RMP-14)	Bio X cell	Cat# BE0146
anti-mouse CTLA-4 (CD152) (9H10)	Bio X cell	Cat# BE0131
Bacterial and Virus Strains		
MAX Efficiency DH5a Competent Cells	Thermo Fisher Scientific	Cat# 18258012
Biological Samples		
Sorted NK cells from WT and $Cd155^{-/-}$ mice	This paper	N/A
Tumor metastatic Lungs	This paper	N/A
Bone marrow from WT and $Cd155^{-/-}$ mice	This paper	N/A
Chemicals, Peptides, and Recombinant Proteins		
Recombinant GM-CSF	Biolegend	Cat# 576306
Recombinant Mouse IL-18	Glaxo Smith Kline	N/A
Recombinant Mouse IL-12	Biolegend	Cat# 577002
Critical Commercial Assays		
$CD8a^{+}$ T Cell Isolation Kit, mouse	Miltenyi Biotec	Cat# 130-104-075
CellTrace Violet Cell Proliferation Kit	Thermofisher	Cat# C34557
NK Cell Isolation Kit II, mouse	Miltenyi Biotec	Cat# 130-096-892
BD CBA Flex Sets	BD Biosciences	
Deposited Data		
Experimental Models: Cell Lines		
B16F10 (melanoma)	ATCC	ATCC® CRL-6475™
B16F10-Cd155ko (sg2/sg6)	This paper	N/A
B16F10-Cd155ko (sg6)-Cd155ova	This paper	N/A
SM1WT1 (melanoma)	Lucas et al. 2014	N/A
LWT1 (melanoma)	Lucas et al. 2014	N/A
LWT1-Cd155ko (sg2/sg6)	This paper	N/A
MC38 (colon cancer)	Kerafast	CVCL_B288
MC38-Cd155ko (sg2/sg6)	This paper	N/A
4T1.2 (breast cancer)	Lelekakis et al. 1999	RRID:CVCL_GR32

4T1.2-Cd155ko (sg2/sg6)	This paper	N/A
MCA1956 (fibrosarcoma)	From Prof. Robert Schreiber	N/A
MCA1956-Cd155ko (sg2/sg6)	This paper	N/A
Experimental Models: Organisms/Strains		
C57BL/6	WEHI and in-house bred	N/A
B6. *Rag2*$^{-/-}$*Il2rγ*$^{-/-}$	Taconic and and in-house bred	N/A
Ptprc^{a}	WEHI and in-house bred	N/A
B6. *Cd155*$^{-/-}$	From Prof. Yoshimi Takai	Back crossed to in-house C57BL/6
BALB/c	WEHI	N/A
B6. *Cd226*$^{-/-}$	Chan et al. 2014	N/A
Oligonucleotides		
mCd155-sgRNA1(sg1)-Forward primer: CACCGCCTCTCCCACCTTGATACTGCAGG	This paper	N/A
mCd155-sgRNA1(sg1)-Reverse primer: AAACCCTGCAGTATCAAGGTGGGAGAGGC	This paper	N/A
mCd155-sgRNA1(sg2)-Forward primer: CACCGCAGCCATGACAGCGGGGAGCGG	This paper	N/A
mCd155-sgRNA1(sg2)-Reverse primer: AAACCCGCTCCCCGCTGTCATGGCTGC	This paper	N/A
mCd155-sgRNA1(sg3)-Forward primer: CACCGTCAGACTACAGTGCAAGGTGG	This paper	N/A
mCd155-sgRNA1(sg3)-Reverse primer: AAACCCACCTTGCACTGTAGTCTGAC	This paper	N/A
mCd155-sgRNA1(sg4)-Forward primer: CACCGTGACTTCCATTCACATTCGAGG	This paper	N/A
mCd155-sgRNA1(sg4)-Reverse primer: AAACCCTCGAATGTGAATGGAAGTCAC	This paper	N/A
mCd155-sgRNA1(sg5)-Forward primer: CACCGAGATGGACACGTTTTCAGGTGG	This paper	N/A
mCd155-sgRNA1(sg5)-Reverse primer: AAACCCACCTGAAAACGTGTCCATCTC	This paper	N/A
mCd155-sgRNA1(sg6)-Forward primer: CACCGTCACCAATGCCCTAGGGTCTGGG	This paper	N/A
mCd155-sgRNA1(sg6)-Reverse primer: AAACCCCAGACCCTAGGGCATTGGTGAC	This paper	N/A

Recombinant DNA		
pX330-U6-Chimeric_BB-CBh-hSpCas9	From Feng Zhang's lab	Addgen Plasmid #42230
PrP-GFP	Gift From Dr. Tobias Bald	N/A
PX330-mCD155-sgRNA2	This paper	N/A
PX330-mCD155-sgRNA6	This paper	N/A
Software and Algorithms		
Graphpad Prism 7 software	GraphPad Software, Inc.	http://www.graphpad.com/scientific-software/prism/
FlowJo V10	FlowJo LLC	www.flowjo.com
Sequence scanner v1.0	ABI	https://products.appliedbiosystems.com/ab/en/US/adirect/ab?cmd=catNavigate2&catID=600583&tab=Overview
IncuCyte ZOOM Plate Map Editor 2016A	Essen Bioscience	https://www.essenbioscience.com/en/products/software/incucyte-base-software/
FCS Express 6 plus Image Cytometry	De Novo Software	https://www.denovosoftware.com/site/WhatsNewInV6.shtml
Vectra 3.0 Automated Quantitative Pathology Imaging System	PerkinElmer	http://www.perkinelmer.com/au/product/vectra-3-0-200-slide-cls142338
Other		